SPANDIDOS PUBLICATIONS

ONCOLOGY LETTERS 14: 5540-5548, 2017

Pteisolic acid G, a novel ent-kaurane diterpenoid, inhibits viability and induces apoptosis in human colorectal carcinoma cells

SHUANGLI QIU[1*], XIN WU[2,3*], HONGBO LIAO[2], XIAOBIN ZENG[2,3], SENWANG ZHANG[2], XIAOFEN LU[2], XIAOHONG HE[2], XIAOQI ZHANG[4], WENCAI YE[4], HUA WU[1] and XIAOHUI ZHU[2]

[1]Cancer Center, The Affiliated Hospital of Guangdong Medical University, Zhanjiang, Guangdong 524001; [2]Guangdong Key Laboratory for Research and Development of Natural Drugs, Guangdong Medical University, Zhanjiang, Guangdong 524023; [3]Key Laboratory for New Drug Research of TCM and Shenzhen Branch, State R&D Centre for Vitro-Biotech, Research Institute of Tsinghua University in Shenzhen, Shenzhen, Guangdong 518057; [4]Institute of Traditional Chinese Medicine and Natural Products, Jinan University, Guangzhou, Guangdong 510632, P.R. China

Received November 23, 2015; Accepted June 27, 2016

DOI: 10.3892/ol.2017.6889

Abstract. Human colorectal cancer (CRC) is a major cause of cancer morbidity and mortality, and its incidence rates are increasing in economical transitioning areas globally. To develop efficient chemotherapy drugs for CRC, the present study isolated and identified a novel *ent*-kaurane diterpenoid from *Pteris semipinnata*, termed pterisolic acid G (PAG). This *ent*-kaurane diterpenoid was demonstrated to significantly inhibit the growth of human CRC HCT116 cells in a time- and dose-dependent manner, determined using the Cell Counting Kit-8 assay. Additionally, western blot analysis, Hoechst 33342 staining and cytometry analysis revealed that PAG not only inhibited the viability of HCT116 cells by suppressing the dishevelled segment polarity protein 2/glycogen synthase kinase 3 β/β-catenin pathway, but also induced the apoptosis of HCT116 cells by downregulating nuclear factor-κB p65 activity, stimulating p53 expression and promoting the generation of intracellular reactive oxygen species. These results suggest that PAG, a novel inhibitor of the Wnt/β-catenin pathway and inducer of apoptosis, should be investigated in more detail using *in vivo* experiments and comprehensive mechanistic studies in order to examine the potential use of PAG as a novel therapeutic agent for the treatment of CRC.

Correspondence to: Dr Hua Wu, Cancer Center, The Affiliated Hospital of Guangdong Medical University, 57 North Renmin Avenue, Zhanjiang, Guangdong 524001, P.R. China
E-mail: zhanjiangwh@126.com

Dr Xiaohui Zhu, Guangdong Key Laboratory for Research and Development of Natural Drugs, Guangdong Medical University, 2 East Wenming Road, Zhanjiang, Guangdong 524023, P.R. China
E-mail: zxh2681731@163.com

*Contributed equally

Key words: ent-kaurane diterpenoid, pterisolic acid G, Wnt/β-catenin pathway, viability, apoptosis

Introduction

Colorectal cancer (CRC) is the third leading cause of morbidity and the fourth cause of mortality in all types of cancer globally, with ~1.2 million new cases and ~600,000 mortalities recorded annually (1). The rate of incidence of CRC has stabilized in the United States and numerous other western countries; however, it is increasing rapidly in economically transitioning areas, including eastern European countries and most parts of Asia (2,3). The increased incidence rate of CRC in economically transitioning areas is thought to be due a shift towards western dietary and lifestyle factors, including a diet rich in unsaturated fats and red meat, increased total energy intake, excessive alcohol consumption and reduced physical activity (4). At present, the majority of patients with early (stage I and II) CRC are treated by surgery to remove the cancer, while patients with late (stage III and IV) CRC often undergo chemotherapy (5), and the toxic effect of chemotherapy remains a challenge (6). Therefore, it is important to clarify the molecular mechanisms underlying the development and progression of CRC in order to develop novel drugs, which may increase the survival rate for patients with CRC.

There are numerous pathways involved in the pathogenesis of CRC, including Wnt/β-catenin, p53, transforming growth factor b, mitogen activated protein kinase, phosphoinositide 3-kinase, epidermal growth factor receptor, Notch, RhoA/rho-associated protein kinase and toll-like receptor (7,8). Hyperactivation of the Wnt/β-catenin signaling pathway is considered to be the most important driving force behind CRC (9). Any genetic defects occurring to members of Wnt/β-catenin pathway, including LDL receptor related protein 5/6, Axin, dishevelled (Dvl), adenomatous polyposis coli (APC), glycogen synthase kinase 3 β and β-catenin, will result in the nuclear accumulation of β-catenin. β-catenin forms complexes with the transcription cofactor T-cell factor (TCF)/lymphoid enhancer factor (LEF) to promote the expression of its target genes (c-Myc, cyclin D1 and survivin) which promotes the initiation and development of CRC (10).

Resistance to apoptosis, caused by an imbalance of pro-apoptotic members including B-cell lymphoma 2 (Bcl-2),

B-cell lymphoma-extra large (Bcl-X_L), myeloid cell leukemia sequence 1 and the anti-apoptotic partners Bcl-2-like protein 11 (Bim), Bcl-2-associated X, apoptosis regulator (Bax), p53-upregulated modulator of apoptosis (Puma), hyperactivation of nuclear factor-κB (NF-κB), inactivation or mutation of p53, or the overexpression of certain oncoproteins (including c-Myc and Ras), are also important factors in the progression of CRC (11,12). Thus, attempts to inverse these abnormal alterations simultaneously represents the rationale behind current strategies for CRC chemotherapy.

As a result of the increase in the use of targeted therapies, studies into the use of natural products as anticancer drugs were abandoned by numerous large pharmaceutical companies between 1997 and 2007. However since 2007, 12 natural product derivatives, including temsirolimus, everolimus, ixabepilone, vinflunine, romidepsin, trabectedin, cabazitaxel, abiraterone acetate, eribulin mesylate, homoharringtonine, carfilzomib and ingenol mebutate, have been approved for the treatment of cancer (13). The discovery of these natural products has encouraged multiple groups to continue the investigation of natural compounds with anticancerous activities. *Ent*-kaurane diterpenoid is a small secondary metabolite molecule with comprehensive antineoplasmic activities, which has attracted the interest of bio-organic chemists (14,15). In a previous study by our group on the active constituents of *Pteris semipinnata*, a traditional Chinese medicine, several *ent*-kaurane diterpenoids were isolated, and their antitumor activities and mechanisms were studied (16).

The present study focused on screening more active *ent*-kaurane diterpenoids from *P. semipinnata* through systemic chemical constituent separation. This separation resulted in the isolation of a novel *ent*-kaurane diterpenoid, termed pterisolic acid G (PAG), which exhibited significant inhibitory effects on the viability of human CRC HCT116 cells. The present study reported the isolation and identification of PAG, as well as the molecular mechanisms behind its activity. The present results demonstrate that PAG is a novel chemotherapeutic agent, which simultaneously inhibits viability and induces apoptosis in human CRC HCT116 cells.

Materials and methods

Materials. The aerial parts, those completely exposed in air, of *P. semipinnata* were collected in Zhangjiang, China, and the identify of these were validated by Professor Zhang-Pin Gou (Department of Pharmacology, Guangdong Medical University, Zhanjiang, China). A voucher specimen (no. 20140812) was deposited in the Guangdong Key Laboratory for Research and Development of Natural Drugs (Zhanjiang, China). RPMI-1640 medium was purchased from Invitrogen; Thermo Fisher Scientific, Inc. (Waltham, MA, USA). Fetal bovine serum (FBS) was obtained from Gibco; Thermo Fisher Scientific, Inc. Propidium iodide (PI) was purchased from Sigma-Aldrich; Merck KGaA (Darmstadt, Germany). Hoechst 33342 was obtained from Beyotime Institute of Biotechnology (Haimen, China).

Antibodies against glycogen synthase kinase-3 (GSK-3β; cat no. 610201; dilution, 1:2,000), GSK-3β (p-Try216; cat no. 612312; dilution, 1:1,000), β-catenin (cat no. 610,154; dilution, 1:1,000) and c-Myc (cat no. 551101; dilution, 1:500) were obtained from BD Biosciences (San Jose, CA, USA). Antibodies against GSK-3β (p-Ser9; cat no. 9322; dilution, 1:2,000), β-actin (cat no. 4967; dilution, 1:3,000), survivin (cat no. 2808; dilution, 1:1,000), Bcl-2 (cat no. 2870; dilution, 1:1,000), Bcl-X_L (cat no. 2764; dilution, 1:1,000), Puma (cat no. 12450; dilution, 1:500) and Bax (cat no. 5023; dilution, 1:1,000) were purchased from Cell Signaling Technology, Inc. (Danvers, MA, USA). Antibodies against Dvl-2 (cat no. sc-13974; dilution, 1:1,000), cyclin D1 (cat no. sc-753; dilution, 1:500) and p53 (cat no. sc-6243; dilution, 1:2,000) were from Santa Cruz Biotechnology, Inc. (Dallas, TX, USA). The histone 3 antibody (cat no. orb136531; dilution, 1:3,000) was bought from Biorbyt, Ltd. (Cambridge, UK). The caspase-3 (pro and active) antibody (cat no. NB100-56708; dilution, 1:2,000) was purchased from Novus Biologicals, LLC (Littleton, CO, USA). Purified anti-poly ADP ribose polymerase (PARP; dilution, 1:2,000) was obtained from BioLegend, Inc. (San Diego, CA, USA). NF-κB-p65 (cat no. 21014; dilution, 1:1,000) and NF-κB-p65 [phospho (p-) Ser536; cat no. 11014; dilution, 1:500] antibodies were purchased from Signalway Antibody LLC (College Park, MD, USA).

General chemi-analysis experiments. Nuclear magnetic resonance (NMR) spectra were recorded using a Bruker AV-500 spectrometer at room temperature, according to the manufacturer's instructions. High-resolution electrospray ionization mass spectrometry data were acquired using an Agilent 6210 liquid chromatography/mass selective detector time-of-flight mass spectrometer (Agilent Technologies, Inc., Santa Clara, CA, USA) at room temperature, according to the manufacturer's instructions. Analytical high-performance liquid chromatography (HPLC) and UV spectra were performed on an Agilent 1200 series and a C_{18} reversed-phase column (4.6x250 mm, 5.0 μM; Cosmosil; Agilent Technologies, Inc.; 25˚C, 1 ml/min, CH_3CN-H_2O, 19:81, v/v), according to the manufacturer's instructions. Preparative HPLC was performed on a Gilson 305 pump, a Varian Prostar 345 UV detector and a C_{18} reversed-phase column (20x250 mm, 5.0 μM; Cosmosil; Agilent Technologies, Inc.; 25˚C, 20 ml/min, CH_3CN-H_2O; 19:81, v/v; internal standards were not used), according to the manufacturer's instructions.

Purification of PAG. The dried aerial sections of *P. semipinnata* (5.0 kg) were powdered and extracted 3 times with 95% ethyl alcohol at room temperature (50 l each time). The solution was concentrated under vacuum at 50˚C to yield 495 g residue. The residue was suspended in distilled water, and subsequently successively partitioned with n-hexane, ethyl acetate (EtOAc) and n-butanol. Following removal of the solvent, 100 g EtOAc extract was subjected to a Sephadex LH-20 column to remove flavonoids using CH_3OH as the eluent. Total terpenoid (TT, 80 g) was yielded upon concentrating the CH_3OH dripped ahead. TT (70 g) was separated by silica gel column eluting with gradient mixtures of $CHCl_3$-CH_3OH (100:0 to 100:20, v/v) to obtain 6 fractions (Fraction A to fraction F). Fraction B (10.5 g) was subjected to chromatography using a reversed-phase C_{18} silica gel column with gradient CH_3OH-H_2O (10:90 to 60:40, v/v) to yield 16 sub-fractions (B1 to B16). PAG (100.3 mg) was further purified by preparative HPLC (CH_3CN-H_2O, 19:81, v/v) from 1.3 g of sub-fraction B9.

Cell culture. Human CRC HCT116 cells (CCL-247; American Type Culture Collection, Manassas, VA, USA) were cultured with RPMI-1640 medium supplemented with 10% heat-inactivated FBS in an atmosphere of 5% CO_2 at 37˚C. Cells were subcultured when they reached 90% confluence.

Cell viability assay. Cell Counting Kit-8 (CCK-8; catalog no. CK04; Dojindo Molecular Technologies, Inc., Kumamoto, Japan) and trypan blue dye exclusion (TBE) assays were used to evaluate the effect of PAG on HCT116 cell viability according to the manufacturer's protocol. Briefly, $2x10^3$ cells were seeded in each well of 96-well microplates and exposed to different concentrations (3.125, 6.25, 12.5, 25, 50 and 100 μM) of PAG for 24, 48 and 72 h. Dimethyl sulfoxdide was added to cells as a negative control. Cellular viability was measured as a percentage of the viability of control cells. At 4 h prior to culture termination, 10 μl CCK-8 reagent was added to each well. After 2-3 h incubation at 37˚C, the optical density was read on a 96-well microplate reader at a wavelength of 490 nm. For the TBE test, a total of $2x10^5$ cells/ml were seeded in 24-well plates and treated with PAG at concentrations of 0, 3.125, 6.25, 12.5 and 25 μM for 24 h. Cells stained with 0.04% trypan blue (catalog no. T8154; Sigma-Aldrich; Merck KGaA) for 5 min at room temperature. Cell numbers were assessed by cell counting under an inverted light microscope (TS100; magnification, x100; Nikon Corporation, Tokyo, Japan). Dead cells were stained blue and live cells were not.

Cell cycle and apoptosis analysis by flow cytometry. Following culture with or without PAG for 24 h, HCT116 cells were pelleted by centrifugation at 200 x g for 5 min at room temperature, washed with PBS, then fixed overnight in 75% ethanol at 4˚C and subsequently washed twice in cold PBS. Prior to fluorescence-activated cell sorting (FACS) analysis using a flow cytometer (Epics, XL-ECL; Beckman Coulter, Inc., Brea, CA, USA), cells were labelled with PI work buffer (1X PBS; 50 μg/ml PI; 2.5 μg/ml RNase) at room temperature for 1 h in the dark. Cell-cycle distribution and apoptosis rate were analyzed with equipped software (EXPO32 ADC software, version 1.1; Beckman Coulter, Inc.).

Hoechst 33342 staining. PAG-treated cells were fixed by a mixture of methanol and glacial acetic acid (v/v, 3:1) at room temperature for 15 min and washed with PBS twice. Hoechst 33342 dye (2.5 μg/ml) was then added, and cells were incubated for 3-5 min in the dark at room temperature. Fluorescent images including 0, 12.5, 25 and 50 μM PAG-triggered apoptotic cells were captured using a fluorescence microscope (DM2500; 200-fold magnification; Leica Microsystems, Inc., Buffalo Grove, IL, USA). The average cell number of a microscopic field was 500-560, and the typical images were selected as representative figures.

Reactive oxygen species (ROS) measurement. Cells were pretreated with 10 μM dichloro-dihydro-fluorescein diacetate (DCFH-DA; S0033; Beyotime Institute of Biotechnology, Haimen, China) in the presence or absence of PAG for 20 min at 37˚C. Cells were then washed 3 times with RPMI-1640 medium and ROS generation was measured by flow cytometry, according to the manufacturer's protocol.

Western blot analysis. Proteins were extracted from the cultured cells using a RIPA lysis buffer supplemented with freshly added 100 mM phenylmethylsulfonyl fluoride on ice for 30 min. The cell lysates were centrifuged at 15,000 x g for 10 min at 4˚C. Supernatants were quantified using a BCA protein assay kit, and total protein (50-80 μg/lane) was subjected to SDS-PAGE (10, 12 or 15% gels), according to the molecular weight of target proteins. Subsequently, protein was transferred to a nitrocellulose membrane and blocked with 5% skim milk at room temperature for 1 h. The membrane was incubated with corresponding primary antibody mentioned above [antibodies against β-catenin, histone 3, β-actin, Dvl-2, p-Try216-GSK-3β, p-Ser9-GSK-3β, GSK-3β, cyclin D1, c-Myc, caspase-3 (pro and active), PARP, survivin, Bcl-2, Bcl-XL, Puma, Bax, Bim, p53, p-Ser536-NF-κB-p65 and NF-κB-p65)] at 4˚C overnight and washed 3 times (10 min each) with PBS-Tween-20 (PBST). Subsequently, the membrane was incubated with peroxidase-conjugated goat anti-rabbit IgG (H+L) secondary antibody (cat no. ZB-2301; dilution, 1:1,000-1:4,000) or peroxidase-conjugated goat anti-mouse IgG (H+L) secondary antibody (cat no. ZB-2305; dilution, 1:1,000-1:4,000) (all from OriGene Technologies, Inc., Rockville, MD, USA) at room temperature for 1 h, washed 2 times with PBST (10 min each) and washed once with PBS. The blots were visualized using enhanced chemiluminescence reagents (WBKLS0050; EMD Millipore, Billerica, MA, USA) in a dark room, followed by developing the blots on X-ray film. β-actin was used as the internal control in western blot analysis.

Statistical analysis. GraphPad Prism 5.0 software (GraphPad Software, Inc., La Jolla, CA, USA) was used to perform the statistical analysis. Comparisons between multiple groups were performed using one-way analysis of variance with Tukey's post hoc intergroup comparisons. $P<0.05$ was considered to indicate a statistically significant difference.

Results

Identification of PAG. The novel compound was obtained as a white amorphous powder (methanol), and had a molecular formula of $C_{20}H_{28}O_6$ as determined by HR-ESI-MS at m/z 387.1816 [M+Na]+(calculated for $C_{20}H_{28}O_6Na$, 387.1778). The UV revealed λ_{max} at 238 nm indicating the presence of an α, β-unsaturated ketone carbonyl chromophore (17). The ^{13}C NMR and DEPT-135 spectra identified 20 carbons, including an α, β-unsaturated ketone group at δ_C 207.0 (C), 154.9 (C) and 116.7 (CH_2), a carboxylic carbon at δ_C 184.4 (C), 2 methyls at δ_C 26.2 (CH_3) and δ_C 19.8 (CH_3), 5 methenes at δ_C 17.9 (CH_2), 25.3 (CH_2), 25.9 (CH_2), 29.3 (CH_2) and δ_C 31.8 (CH_2), 6 methines at δ_C 47.5 (CH), 46.0 (CH), 36.8 (CH), 70.8 (OCH), 71.6 (OCH) and 85.4 (OCH), and 3 quaternary carbons at δ_C 40.2 (C), 42.5 (C) and δ_C 56.3 (C).

The ^1H-NMR spectrum exhibited legible signals as follows: 2 olefinic protons at δ_H 5.86, 5.41 (each broad singlet) due to an exocyclic methylene group, 3 oxygenated methine protons at δ_H 3.50 (1H, d, J=3.2 Hz), 4.27 (1H, d, J=5.6 Hz) and 5.21 (1H, d, J=5.8 Hz), and 2 methyl singlets at δ_H 1.30 (3H, s) and 0.77 (3H, s). The aforementioned structural features revealed that the compound should be a 15-oxo-*ent*-kuar-16-en-19-oic acid derivative (18).

With the aid of ^{1}H-^{1}H correlation spectroscopy (COSY), heteronuclear single quantum coherence spectroscopy and heteronuclear multiple bond correlation (HMBC) experiments, all the ^{1}H and ^{13}C NMR signals were assigned as presented in Table I. The HMBC correlations between δ_H 3.50 (H-1) and δ_C 19.8 (C-20)/25.3 (C-3)/47.5 (C-5)/40.2 (C-10); between δ_H 5.21 (H-6) and δ_C 40.2 (C-10)/47.5 (C-5)/71.6 (C-7); and between δ_H 4.27 (H-7) and δ_C 207.0 (C-15)/29.3 (C-14)/56.3 (C-8)/85.4 (C-6), revealed the presence of hydroxy groups at C-1, C-6 and C-7, respectively. The assignment of C19-oic acid was further confirmed by the HMBC correlations between δ_H 1.30 (H-18)/1.61 (H-3)/1.98 (H-3)/2.31 (H-5) and δ_C 184.4 (C-19). Determined using the Bruker AV-500 spectrometer, the ^{13}C chemical shift of 18-CH_3 at δ 26.2 suggested its β-orientation (19) (α-18-CH_3 at ~δ16.7) (20), which was supported by the absence of rotational overhauser effect spectroscopy (ROESY) correlation between δ_H 1.04 (Me-20) and δ_H 1.39 (Me-18). The ROESY correlations between H-5 and H-9, and H-9 and H-1 indicated that these protons were cofacial and β-oriented. The β-H-6 and *α*-H-7 orientations were confirmed by ROESY correlations between H-6 and Me-18, and H-7 and Me-20, respectively. Detailed key ^{1}H-^{1}H COSY, HMBC and ROESY information is presented in Fig. 1A and B. Accordingly, the structure of the compound was elucidated as *ent*-1β, 6α, 7β-trihydroxy-15-oxo-9 (11), 16-kauradien-19α-oic acid, and termed PAG (Fig. 1A).

PAG inhibits the viability of HCT116 cells. The inhibitory effect of PAG on HCT116 cell viability was measured using a CCK-8 assay and a TBE test. As presented in Fig. 1C, PAG exhibited significant cytotoxicity to HCT116 cells in a dose- and time-dependent manner with IC_{50} values at 20.43, 16.15 and 4.07 μM for 24, 48 and 72 h, respectively. The results of the TBE assay also demonstrated that PAG sharply induced HCT116 cellular death in a concentration-dependent manner following 24 and 48 h treatment (Fig. 1D). At 72 h, no stained cells were observed since the cells were lysed by PAG (data not shown).

Effects of PAG on the cell cycle and apoptosis in HCT116 cells. The present study subsequently explored whether the cell cycle and apoptosis were affected by PAG using FACS analysis following PI staining. The results revealed that PAG affected cell cycle distributions without a clear dose-dependent effect overall. However, it was worth noting that PAG markedly increased the S population at 25 and 50 μM following 24 h treatment. Analysis of apoptosis revealed dose-dependent apoptotic cell death in HCT116 cells following PAG treatment (Fig. 2A). Taking these low percentages of apoptosis detected by flow cytometry into consideration, the rate of apoptosis was then observed by fluorescence microscopy subsequent to staining with Hoechst 33342 dye. As presented in Fig. 2B, blue fluorescence in HCT116 cells treated with the same concentrations of PAG as FACS analysis for 24 h was visibly increased. Together, these results demonstrated that PAG induced cellular apoptosis in HCT116 cells.

PAG suppresses the Dvl-2/GSK-3β/β-catenin pathway in HCT116 cells. From the aforementioned information, it was clear that PAG significantly inhibited cellular viability in HCT116 cells, however the mechanisms behind this remain unclear. Previously, two *ent*-kaurane diterpenoids have been reported to execute antitumor functions in CRC cell lines by inhibiting the Wnt/β-catenin pathway (21,22). This led the present study to investigate the interference of PAG on this signaling. Therefore, nuclear, cytoplasmic and total β-catenin, as well as its target proteins c-Myc and cyclin D1, were detected by western blot analysis. The results demonstrated that nuclear and total β-catenin, along with c-Myc and cyclin D1, were decreased by PAG in a dose-dependent manner, while cytoplasmic β-catenin was not detected by western blot analysis in all 3 treated concentrations of PAG, compared with the untreated control (Fig. 3).

These results suggested that PAG may depress nuclear accumulation and decrease the total content of β-catenin by promoting cytoplasmic β-catenin degradation to inhibit cell viability. β-catenin degradation is initiated by amino-terminal serine/threonine phosphorylation, which is performed by GSK-3β in a complex with the tumor suppressor proteins (Axin), APC and casein kinase-1α (CK1α) (23). Therefore, further investigations were performed in order to evaluate the effects of PAG on GSK-3β, p-Ser9-GSK-3β (inhibitory form of

Table I. ^{1}H NMR and ^{13}C NMR spectroscopic data of PAG (CD_3OD, *J* in Hz).

Position	δ_C	δ_H
1	70.8 CH	3.50 (t, 3.2)
2	25.9 CH_2	1.73 (m)
		1.50 (m)
3	25.3 CH_2	1.98 (ddd, 14.4, 6.5, 2.6)
		1.61 (m)
4	42.5 C	-
5	47.5 CH	2.31 (d, 6.0)
6	85.4 CH	5.21 (d, 5.8)
7	71.6 CH	4.27 (d, 5.6)
8	56.3 C	-
9	46.0 CH	1.92 (dd, 13.1, 4.3)
10	40.2 C	-
11	17.9 CH_2	1.54 (m)
		1.59 (m)
12	31.8 CH_2	1.50 (m)
		2.28 (m)
13	36.8 CH	3.02 (dd, 9.1, 4.5)
14	29.3 CH_2	2.02 (d, 11.8)
		2.08 (dd, 11.9, 4.6)
15	207.0 C	-
16	154.9 C	-
17	116.7 CH_2	5.86 (s)
		5.41 (s)
18	26.2 CH_3	1.30 (s)
19	184.4 C	-
20	19.8 CH_3	0.77 (s)

NMR, nuclear magnetic resonance; t, triple; m, multiple; d, double; dd, double-double; s, single.

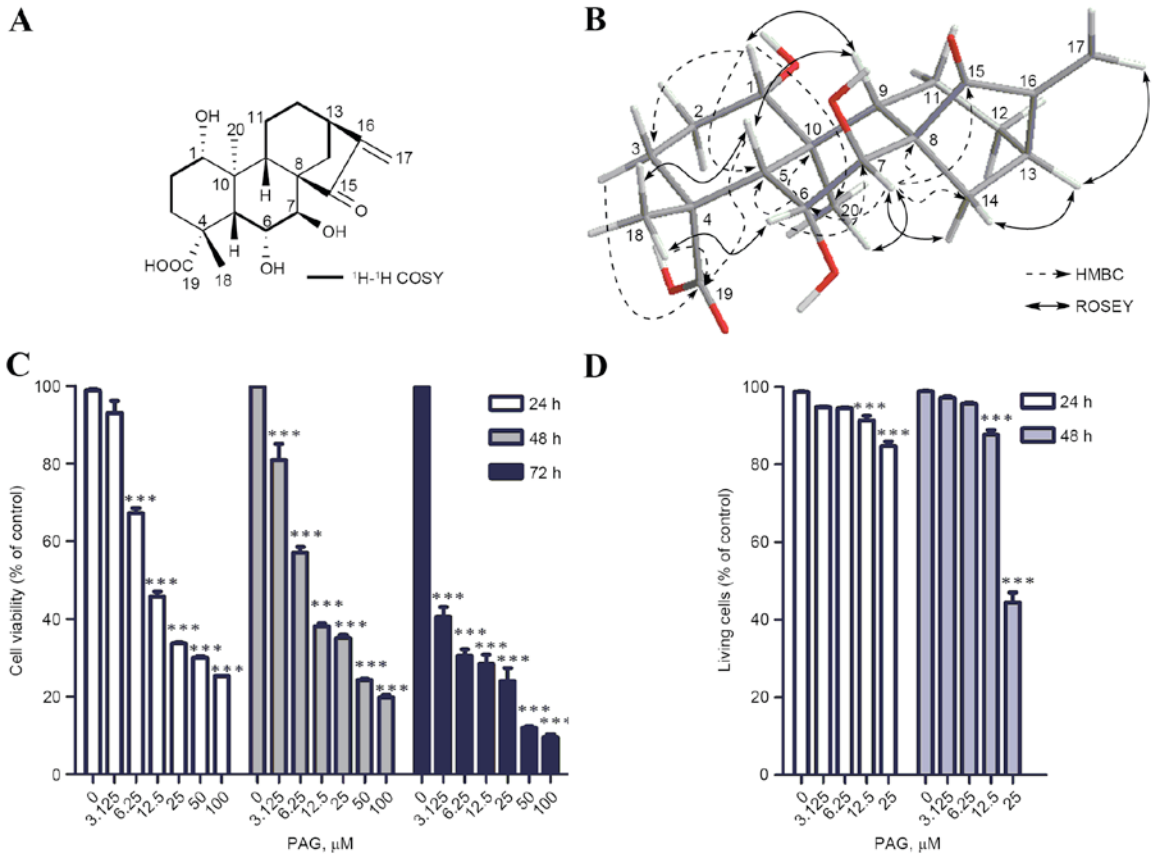

Figure 1. PAG reduces HCT116 cell viability. (A) Chemical structure of PAG and its ^{1}H-^{1}H COSY correlations. (B) Key HMBC and ROESY correlations of PAG. (C) The viability of HCT116 cells treated with indicated concentrations of PAG for 24, 48 or 72 h, as assessed by Cell Counting Kit-8. (D) Cells were treated with increasing concentrations of PAG for 24 and 48 h, and the ratio of dead cells to living cells was determined by a trypan blue exclusion assay. Data are presented as the mean ± standard deviation of 3 independent experiments. ***P<0.001 vs. untreated cells. PAG, pterisolic acid G; HMBC, heteronuclear multiple bond correlation; ROESY, rotational overhauser effect spectroscopy.

GSK-3β) and p-Tyr216-GSK-3β (active form of GSK-3β) (24). The upregulation of GSK-3β and p-Tyr216-GSK-3β, and the downregulation of p-Ser9-GSK-3β (Fig. 3) implied that PAG enhanced GSK-3β activity. The recruitment of Dvl to Frizzled may result in the deactivation of GSK-3β by phosphorylation of Ser9 and the dephosphorylation of Tyr216 (25,26), resulting in the disassembly of the β-catenin destruction complex (Axin/APC/GSK-3β/CK1α) (27), ultimately leading to the nuclear accumulation of β-catenin in the canonical Wnt/β-catenin pathway. The effect of PAG on Dvl-2 was then examined. The results revealed that PAG downregulated Dvl-2 protein levels (Fig. 3). In summary, the present results indicated that PAG inhibited the viability of HCT116 cells by suppressing the Dvl-2/GSK-3β/β-catenin pathway.

Mechanisms underlying cellular apoptosis induced by PAG. Western blot analysis revealed an increase in the cleavage of PARP (85 kDa) and active-caspase-3 (17 kDa) in a concentration-dependent manner by PAG, which coincided with the decline of PARP (116 kDa) and pro-caspase-3 (35 kDa; Fig. 4A), and confirmed the presence of caspase-dependent apoptosis. To investigate how PAG induced the apoptosis of HCT116 cells, investigations were performed on apoptosis-associated proteins. As presented in Fig. 4B, PAG decreased the levels of anti-apoptotic proteins including survivin, Bcl-2 and Bcl-X_L, and increased the levels of pro-apoptosis proteins including Puma, Bax and Bim. The decrease of the anti-apoptotic factors NF-κB p65 and p-p65, as well as the increase of a the tumour suppressor p53, were also detected following PAG treatment (Fig. 4C).

Additionally, DCFH-DA detection was performed following PAG treatment, since it has been previously demonstrated that *ent*-kaurane diterpenoid induces apoptosis by increasing intracellular ROS generation (28). The increase of intracellular ROS levels by PAG in a concentration-dependent manner (Fig. 4D) confirmed this result. In summary, the results of the present study suggested that PAG induced cellular apoptosis in HCT116 cells by decreasing NF-κB p65 activity, increasing p53 expression and promoting the generation of ROS.

Discussion

Over the past decades, chemotherapy techniques for metastatic (m) CRC has developed from the use of a single agent to a combination of cytotoxic therapies and target-specific agents. Although the median survival time has improved, the 5-year overall survival rate for patients with mCRC remains poor (6). Therefore, it is important to develop effective therapeutic agents for the treatment of CRC, particularly mCRC.

The screening of small molecule inhibitors of the Wnt/β-catenin signaling pathway is regarded as a

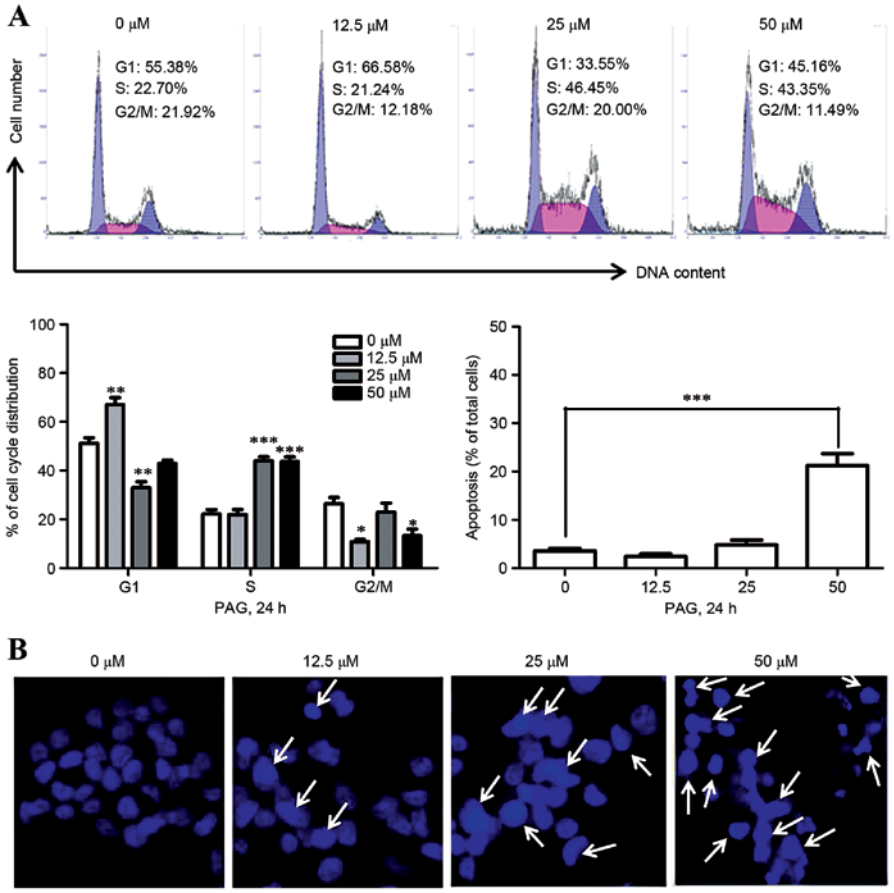

Figure 2. Effects of PAG on cell cycle and apoptosis in human colon carcinoma HCT116 cells. (A) Cell cycle distribution was analyzed by flow cytometry following exposure to PAG for 24 h and propidium iodide staining. (B) Cell apoptosis was analyzed by Hoechst 33342 staining following treatment with PAG for 24 h (magnification, x200). Data are presented as the mean ± standard deviation of 3 independent experiments. *P<0.05, **P<0.01, ***P<0.001 vs. untreated cells. PAG, pterisolic acid G.

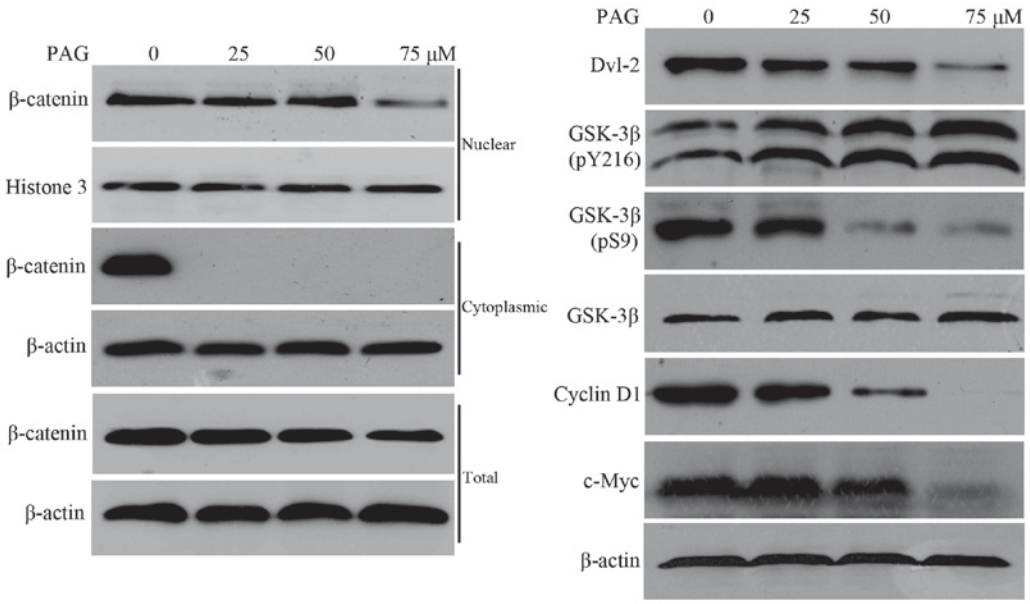

Figure 3. PAG inhibited the Dvl-2/GSK-3β/β-catenin pathway in human colon carcinoma HCT116 cells. Western blot analysis of Wnt/β-catenin signaling components and its target proteins in HCT116 cells treated with indicated concentrations of PAG for 24 h. β-actin was used as a control. PAG, pterisolic acid G; Dvl-2, dishevelled-2; GSK-3β, glycogen synthase kinase-3.

promising strategy for CRC chemotherapy, since the ectopic activation of this pathway is involved in CRC pathogenesis and development (29). Theoretically, these small molecule inhibitors achieve their effect by targeting cytoplasmic proteins

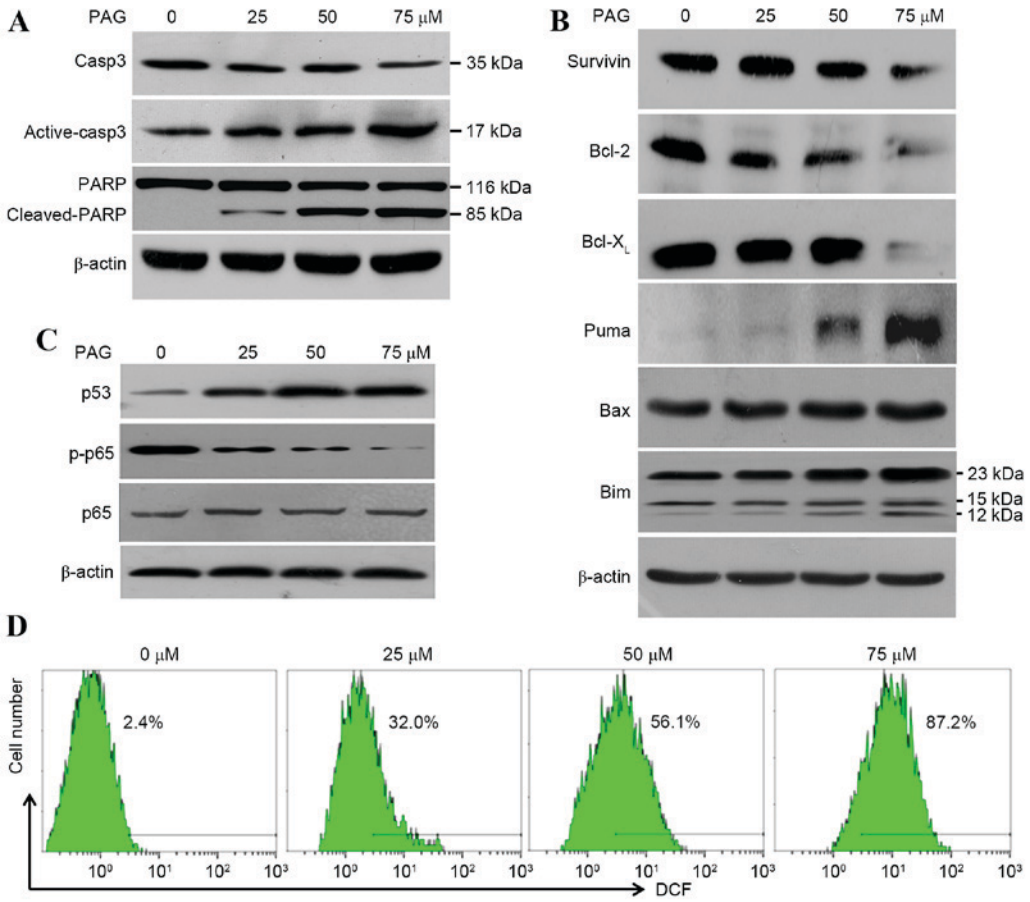

Figure 4. PAG triggered cellular apoptosis in HCT116 cells by increasing p53 expression, decreasing NF-κB p65 activity and promoting the generation of ROS. Cells were exposed to PAG at the indicated concentrations for 24 h. Cell lysates were analyzed by (A) western blot for markers, (B) associated proteins and (C) inducers of apoptosis. (D) Cells treated with 0, 25, 50 and 75 μM PAG for 6 h were stained with dichloro-dihydro-fluorescein diacetate, and the ROS levels were measured by flow cytometry. β-actin was used as a control. PAG, pterisolic acid G; ROS, reactive oxygen species; Casp3, caspase 3; PARP, poly ADP ribose polymerase; p-, phosphorylated; Bcl-2, B-cell lymphoma-2; Bcl-X_L, B-cell lymphoma-extra large; Puma, p53-upregulated modulator of apoptosis; Bax, Bcl-2-associated X, apoptosis regulator; Bim, Bcl-2-like protein 11.

(Dvl, Tankyrase, Porcupine, CK1, Axin, APC and GSK-3), transcriptional factors (TCF/LEF) or co-activators (CBP, p300, Pygo, Bcl-9) of the Wnt/β-catenin cascade. A number of synthetic compounds targeting the Wnt/β-catenin signaling pathway have been identified, and a number of these have been subject to clinical trials (30). Natural products including ginsenosides (31), berberine (32), hydnocarpin (33), murrayafoline A (34), tetrandrine, curcumin, epigallocatechin gallate, baicalin, magnolol and resveratrol (35), are also antagonists of the Wnt/β-catenin signaling pathway. *Ent*-kaurane diterpenoids, 11α, 12α-epoxyleukamenin E (21) and Henryin (22), isolated from *Isodon rubescens var. lushanensis* and *Salvia cavaleriei*, respectively, are able to interfere with the Wnt/β-catenin signaling pathway by impairing β-catenin/TCF4 transcriptional complexes, exerting antitumor activities in CRC cells.

Similarly, the novel *ent*-kaurane diterpenoid PAG identified in the present study may also disrupt the same pathway to exhibit its antineoplastic effect; however, the exact mechanism behind this may differ from what has been indicated in previous studies. The present study revealed that PAG decreases nuclear accumulation and promotes cytoplasmic degradation of β-catenin by decreasing Dvl-2 expression and increasing GSK-3β activity. This suggests that PAG inhibited the viability of HCT116 cells by suppressing the Dvl-2/GSK-3β/β-catenin pathway.

Targeting apoptosis pathways is also an effective method for cancer chemotherapy (36). A number of antitumor agents promote cancer cell apoptosis via NF-κB, p53, ROS, death receptor, phosphatase and tensin homolog, genotoxicity and T lymphocyte cytotoxicity (37). Activated NF-κB suppresses apoptosis by enhancing the expression of anti-apoptotic genes, including Bcl-X_L, X-inhibitor of apoptosis protein (IAP), IAP1, IAP2, radiation-inducible immediate-early gene-1 L and the Bcl-2 family member Bfl-1, which in turn results in an advancement in tumor development (38,39). Based on this, the pro-apoptotic function of PAG may be partially due to the resultant decreased NF-κB p65 and p-p65 expression. In contrast to NF-κB, p53 promotes apoptosis by inducing the expression of Bcl-2 family members and increasing the permeability of the outer membrane of the mitochondria (12,40,41). Therefore, increased p53 expression in HCT116 cells may also contribute to the pro-apoptotic effect of PAG. ROS overexpression, which triggers cell apoptosis, necrosis or autophagy, is a mechanism common to all non-surgical therapeutic approaches for cancers, including chemotherapy, radiotherapy and photodynamic therapy (42). Thus, the PAG-induced increase of intracellular ROS levels may be associated with

its pro-apoptosis activity. In general, PAG induces cellular apoptosis of HCT116 cells by suppressing NF-κB p65 activity, stimulating p53 expression and promoting ROS generation.

In conclusion, the present study purified a novel *ent*-kaurane diterpenoid, PAG, from *P. semipinnata* and investigated its anti-neoplastic activities in human CRC HCT116 cells. Mechanistic studies revealed that PAG not only inhibited the viability of HCT116 cells by suppressing the Dvl-2/GSK-3β/β-catenin pathway, but also induced apoptosis of HCT116 cells by stimulating p53 expression, downregulating NF-κB p65 activation and promoting intracellular ROS generation. The results of the present study suggested that PAG, as a novel inhibitor of the Wnt/β-catenin pathway and inducer of apoptosis, should be further investigated via *in vivo* experiments and comprehensive mechanistic studies in order to examine its potential use as a novel therapeutic agent for the treatment of CRC.

Acknowledgements

The present study was supported by grants from the National Science and Technology Pillar Program of China (grant no. 2013BAI11B05), the National Natural Science Foundation of China (grant no. 81503221 and 81503226), the Shenzhen Technology Development Project (grant no. CXZZ20150402 104158173) and the Undergraduates 'Climbing' Program of Guangdong Province (grant no. pdjh2015b0299).

References

1. Brenner H, Kloor M and Pox CP: Colorectal cancer. Lancet 383: 1490-1502, 2014.
2. Center MM, Jemal A and Ward E: International trends in colorectal cancer incidence rates. Cancer Epidemiol Biomarkers Prev 18: 1688-1694, 2009.
3. Jemal A, Center MM, DeSantis C and Ward EM: Global patterns of cancer incidence and mortality rates and trends. Cancer Epidemiol Biomarkers Prev 19: 1893-1907, 2010.
4. Fearon ER: Molecular genetics of colorectal cancer. Annu Rev Pathol 6: 479-507, 2011.
5. DeSantis CE, Lin CC, Mariotto AB, Siegel RL, Stein KD, Kramer JL, Alteri R, Robbins AS and Jemal A: Cancer treatment and survivorship statistics, 2014. CA Cancer J Clin 64: 252-271, 2014.
6. Merla A and Goel S: Novel drugs targeting the epidermal growth factor receptor and its downstream pathways in the treatment of colorectal cancer: A systematic review. Chemother Res Pract 2012: 387172, 2012.
7. Perkins G and Laurent-Puig P: Colorectal cancer biology. Rev Prat 65: 802-806, 2015 (In French).
8. Zeng Y, Xie H, Qiao Y, Wang J, Zhu X, He G, Li Y, Ren X, Wang F, Liang L and Ding Y: FMNL2 regulates Rho/ROCK pathway to promote actin assembly and cell invasion of colorectal cancer. Cancer Sci 106: 1385-1393, 2015.
9. Jiang X, Tan J, Li J, Kivimäe S, Yang X, Zhuang L, Lee PL, Chan MT, Stanton LW, Liu ET, *et al*: DACT3 is an epigenetic regulator of Wnt/beta-catenin signaling in colorectal cancer and is a therapeutic target of histone modifications. Cancer Cell 13: 529-541, 2008.
10. Cancer Genome Atlas Network: Comprehensive molecular characterization of human colon and rectal cancer. Nature 487: 330-337, 2012.
11. Hanahan D and Weinberg RA: Hallmarks of cancer: The next generation. Cell 144: 646-674, 2011.
12. Meek DW: Regulation of the p53 response and its relationship to cancer. Biochem J 469: 325-346, 2015.
13. Basmadjian C, Zhao Q, Bentouhami E, Djehal A, Nebigil CG, Johnson RA, Serova M, de Gramont A, Faivre S, Raymond E and Désaubry LG: Cancer wars: Natural products strike back. Front Chem 2: 20, 2014.
14. Liu CX, Yin QQ, Zhou HC, Wu YL, Pu JX, Xia L, Liu W, Huang X, Jiang T, Wu MX, *et al*: Adenanthin targets peroxiredoxin I and II to induce differentiation of leukemic cells. Nat Chem Biol 8: 486-493, 2012.
15. Sun HD, Huang SX and Han QB: Diterpenoids from *Isodon* species and their biological activities. Nat Prod Rep 23: 673-698, 2006.
16. Ye H, Liang NC and Zheng XB: Progress in research on anti-tumor effect of 5F isolated from *Pteris semipinnata* L. Nat Pro Res Dev 26: 2082-2087, 2014.
17. Schubert WM and Sweeney WA: The effect of ring strain on the ultraviolet spectra of α,β-unsaturated carbonyl compounds. J Am Chem Soc 77: 2297-2300, 1955.
18. Wang F, Li YJ, Ren FC, Wei GZ and Liu JK: Pterisolic acids A-F, new ent-kaurane diterpenoids from the fern *Pteris semipinnata*. Chem Pharm Bull (Tokyo) 59: 484-487, 2011.
19. Hutchison M, Lewer P and MacMillan J: Carbon-13 nuclear magnetic resonance spectra of eighteen derivatives of ent-kaur-16-en-19-oic acid. J Chem Soc, Perkin Trans 1: 2363-2366, 1984.
20. Santos HS, Barros FW, Albuquerque MR, Bandeira PN, Pessoa C, Braz-Filho R, Monte FJ, Leal-Cardoso JH and Lemos TL: Cytotoxic diterpenoids from *Croton argyrophylloides*. J Nat Prod 72: 1884-1887, 2009.
21. Ye Q, Yao G, Zhang M, Guo G, Hu Y, Jiang J, Cheng L, Shi J, Li H, Zhang Y and Liu H: A novel ent-kaurane diterpenoid executes antitumor function in colorectal cancer cells by inhibiting Wnt/β-catenin signaling. Carcinogenesis 36: 318-326, 2015.
22. Li X, Pu J, Jiang S, Su J, Kong L, Mao B, Sun H and Li Y: Henryin, an ent-kaurane diterpenoid, inhibits Wnt signaling through interference with β-catenin/TCF4 interaction in colorectal cancer cells. PLoS One 8: e68525, 2013.
23. Liu C, Li Y, Semenov M, Han C, Baeg GH, Tan Y, Zhang Z, Lin X and He X: Control of beta-catenin phosphorylation/degradation by a dual-kinase mechanism. Cell 108: 837-847, 2002.
24. Jin Y, Kanno T and Nishizaki T: Acute restraint stress impairs induction of long-term potentiation by activating GSK-3β. Neurochem Res 40: 36-40, 2015.
25. Aschenbach WG, Ho RC, Sakamoto K, Fujii N, Li Y, Kim YB, Hirshman MF and Goodyear LJ: Regulation of dishevelled and beta-catenin in rat skeletal muscle: An alternative exercise-induced GSK-3beta signaling pathway. Am J Physiol Endocrinol Metab 291: E152-E158, 2006.
26. Kim S, Lee J, Park J and Chung J: BP75, bromodomain-containing M(r) 75,000 protein, binds dishevelled-1 and enhances Wnt signaling by inactivating glycogen synthase kinase-3 beta. Cancer Res 63: 4792-4795, 2003.
27. Gao C and Chen YG: Dishevelled: The hub of Wnt signaling. Cell Signal 22: 717-727, 2010.
28. Liao YJ, Bai HY, Li ZH, Zou J, Chen JW, Zheng F, Zhang JX, Mai SJ, Zeng MS, Sun HD, *et al*: Longikaurin A, a natural ent-kaurane, induces G2/M phase arrest via downregulation of Skp2 and apoptosis induction through ROS/JNK/c-Jun pathway in hepatocellular carcinoma cells. Cell Death Dis 5: e1137, 2014.
29. Weng W, Feng J, Qin H and Ma Y: Molecular therapy of colorectal cancer: Progress and future directions. Int J Cancer 136: 493-502, 2015.
30. Zhang X and Hao J: Development of anticancer agents targeting the Wnt/β-catenin signaling. Am J Cancer Res 5: 2344-2360, 2015.
31. Bi X, Xia X, Mou T, Jiang B, Fan D, Wang P, Liu Y, Hou Y and Zhao Y: Anti-tumor activity of three ginsenoside derivatives in lung cancer is associated with Wnt/β-catenin signaling inhibition. Eur J Pharmacol 742: 145-152, 2014.
32. Albring KF, Weidemuller J, Mittag S, Weiske J, Friedrich K, Geroni MC, Lombardi P and Huber O: Berberine acts as a natural inhibitor of Wnt/β-catenin signaling-identification of more active 13-arylalkyl derivatives. Biofactors 39: 652-662, 2013.
33. Lee MA, Kim WK, Park HJ, Kang SS and Lee SK: Anti-proliferative activity of hydnocarpin, a natural lignan, is associated with the suppression of Wnt/β-catenin signaling pathway in colon cancer cells. Bioorg Med Chem Lett 23: 5511-5514, 2013.
34. Choi H, Gwak J, Cho M, Ryu MJ, Lee JH, Kim SK, Kim YH, Lee GW, Yun MY, Cuong NM, *et al*: Murrayafoline A attenuates the Wnt/beta-catenin pathway by promoting the degradation of intracellular beta-catenin proteins. Biochem Biophys Res Commun 391: 915-920, 2010.
35. Tarapore RS, Siddiqui IA and Mukhtar H: Modulation of Wnt/β-catenin signaling pathway by bioactive food components. Carcinogenesis 33: 483-491, 2012.

36. Bai L and Wang S: Targeting apoptosis pathways for new cancer therapeutics. Annu Rev Med 65: 139-155, 2014.
37. Sun SY, Hail N Jr and Lotan R: Apoptosis as a novel target for cancer chemoprevention. J Natl Cancer Inst 96: 662-672, 2004.
38. Kucharczak J, Simmons MJ, Fan Y and Gelinas C: To be, or not to be: NF-kappaB is the answer-role of Rel/NF-kappaB in the regulation of apoptosis. Oncogene 22: 8961-8982, 2003.
39. Lin A and Karin M: NF-kappaB in cancer: A marked target. Semin Cancer Biol 13: 107-114, 2003.
40. Li XL, Zhou J, Chen ZR and Chng WJ: P53 mutations in colorectal cancer-molecular pathogenesis and pharmacological reactivation. World J Gastroenterol 21: 84-93, 2015.
41. Dashzeveg N and Yoshida K: Cell death decision by p53 via control of the mitochondrial membrane. Cancer Lett 367: 108-112, 2015.
42. Wang J and Yi J: Cancer cell killing via ROS: To increase or decrease, that is the question. Cancer Biol Ther 7: 1875-1884, 2008.